# Doppler tomography of the circumstellar disk of π Aquarii.

By: S.V. Zharikov, A.S. Miroshnichenko, E. Pollmann, S. Danford, K.S. Bjorkman, N.D. Morrison, A. Favaro, J. Guarro Fló, J. N. Terry, V. Desnoux, T. Garrel, G. Martineau, Y. Buchet, S. Ubaud, B. Mauclaire, H. Kalbermatten, C. Buil, C.J. Sawicki, T. Blank, O. Garde

Zharikov, S.V.; Miroshnichenko, A.S.; Pollmann, E.; Danford, S.; Bjorkman, K.S.; Morrison, N.D.; Favaro, A.; Guarro Fló, J.; Terry, J.N.; Desnoux, V.; Garrel, T.; Martineau, G.; Buchet, Y.; Ubaud, S.; Mauclaire, B.; Kalbermatten, H.; Buil, C.; Sawicki, C.J.; Blank, T.; Garde, O. Doppler tomography of the circumstellar disk of π Aquarii. *Astronomy & Astrophysics.* [Online] **2013** *560,* A30.

*Astronomy & Astrophysics* manuscript no. szharikovV4
December 5, 2013




# Doppler tomography of the circumstellar disk of $\pi$ Aquarii.

S. V. Zharikov[1], A. S. Miroshnichenko[2], E. Pollmann[3], S. Danford[2], K. S. Bjorkman[4], N. D. Morrison[4], A. Favaro[5], J. Guarro Fló[6], J. N. Terry[7], V. Desnoux[8], T. Garrel[9], G. Martineau[10], Y. Buchet[10], S. Ubaud[11], B. Mauclaire[12], H. Kalbermatten[13], C. Buil[14], C. J. Sawicki[15], T. Blank[16], O. Garde[17]

[1] Observatorio Astronomico Nacional, Instituto de Astronomia, Universidad Nacional Autonoma de Mexico, Ensenada, BC, Mexico e-mail: zhar@astrosen.unam.mx
[2] University of North Carolina at Greensboro, Greensboro, NC 27402, U.S.A. e-mail: a_mirosh@uncg.edu
[3] Emil-Nolde-Str. 12, 51375, Leverkusen, Germany
[4] Ritter Observatory, University of Toledo, Toledo, OH 43606, U.S.A
[5] 19 Boulevard Carnot, 21000 Dijon, France
[6] Balmes, 2, 08784, Piera (Barcelona), Spain
[7] 6 rue Virgile, 42100, Saint-Etienne, France
[8] ARAS, Astronomical Ring for Access to Spectroscopy, http://www.astrosurf.com/aras/, France
[9] Observatoire de Juvignac, 19 avenue du Hameau du Golf 34990, Juvignac, France
[10] SAPP, CSC des Trois CitÉs, Le Clos Gaultier, 86000, Poitiers, France
[11] 16 Calade, St. Roch, 06410, Biot, France
[12] Observatoire du Val de l'Arc, route de Peynier 13530, Trets, France
[13] Ebnetstrasse 12, CH-Bitsch, Switzerland
[14] Castanet Tolosan Observatory, 6 place Clémence Isaure 31320 Castanet Tolosan, France
[15] Alpha Observatory, Alpine, Texas 79830, U.S.A.
[16] Dorfstrasse 3f, 8603, Schwerzenbach, Switzerland
[17] Observatoire de la Tourbiére, 38690, Chabons, France

Received - ; accepted -

**ABSTRACT**

*Aims.* The work is aimed at a study of the circumstellar disk of the bright classical binary Be star $\pi$ Aqr.
*Methods.* We analysed variations of a double-peaked profile of the $H_\alpha$ emission line in the spectrum of $\pi$ Aqr that was observed in many phases during $\sim$ 40 orbital cycles in 2004–2013. We applied the Discrete Fourier Transform (DFT) method to search for periodicity in the peak intensity (V/R) ratio. Doppler tomography was used to study the structure of the disk around the primary.
*Results.* The dominant frequency in the power spectrum of the $H_\alpha$ V/R ratio is 0.011873 day$^{-1}$ that correspond to a period of 84.2(2) days and is in agreement with the earlier determined orbital period of the system, $P_{orb}$ = 84.1 days. The V/R ratio shows a sinusoidal variation phase-locked with the orbital period. Doppler maps of all our spectra show a non-uniform structure of the disk around the primary: a ring with the inner and outer radii at $V_{in} \approx 450$ km s$^{-1}$ and $V_{out} \approx 200$ km s$^{-1}$, respectively, along with an extended stable region (spot) at $V_x \approx 225$ km s$^{-1}$ and $V_y \approx 100$ km s$^{-1}$. The disk radius of $\approx 65R_\odot = 0.33$ AU was estimated assuming Keplerian motion of a particle on a circular orbit at the disk outer edge.

**Key words.** binaries: spectroscopic — circumstellar matter — stars: emission-line, Be — stars: individual ($\pi$ Aquarii) — techniques: spectroscopic.

## 1. Introduction

Classical Be stars are fast-rotating non-supergiant B-type stars with Balmer emission lines in their spectra. The emission lines are recombination lines that occur in a geometrically thin, equatorial, circumstellar disk, according to a model first proposed by Struve (1931). The model has been modified and further developed by many authors and recently confirmed by direct interferometric observations (Quirrenbach et al. 1997; Gies et al. 2007; Carciofi et al. 2009; Grzenia et al. 2013). The disk may entirely disappear and re-appear unpredictably. The intensity of the emission lines varies on a time scale of days to decades. It is widely accepted that the origin of the variability is caused by processes occurring in the circumstellar disk and non-radial pulsations of the B-star photosphere (Porter & Rivinius 2003). Typically the dominant feature in the Be star spectra is an asymmetric double-peaked $H_\alpha$ emission line.

Many Be stars exhibit variations in the ratio of the blue (violet) and red emission peaks (V/R variations) of the Balmer emission lines on a time scale of a few years. V/R variations may be due to the evolution of a one-armed spiral density pattern and/or binary effects (Kato 1983; Okazaki 1991, 1997). The main observational properties of the V/R variations and theoretical suggestions were summarized in Mennickent et al. (1997). The most complete compilation of Be stars showing the V/R variations contains 62 objects (Okazaki 1997). Eleven of them were known to be binaries at the time. The time scale of the V/R variations is typically much longer than rotational periods of the star or the disk and does not correlate with orbital periods of the binaries. However, some binary systems, $\varphi$ Per (Bozic et al. 1995; Gies et al. 1998), V696 Mon (Peters 1972), 4 Her (Harmanec et al. 1976; Koubsky et al. 1997), V744 Her (Doazan et al. 1982), $\kappa$ Dra (Juza et al. 1991),

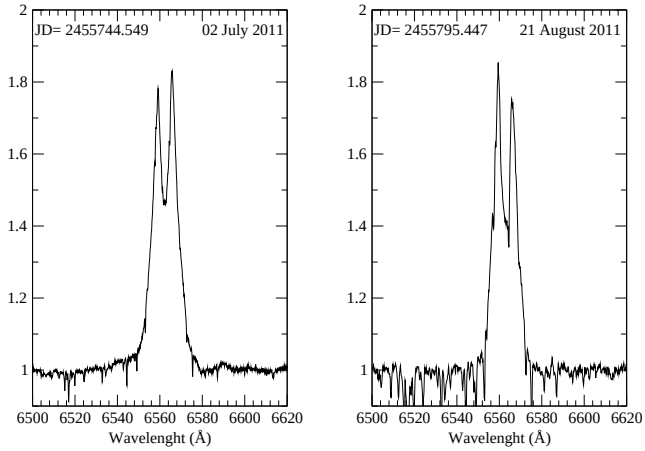


**Fig. 1.** V and R dominated examples of $\pi$ Aqr $H_\alpha$ profiles. Epoch of observations are shown.

$\epsilon$ Cap (Rivinius et al. 1999) and FY CMa (Rivinius et al. 2004) present an exception from the rule. For example, in the case of 4 Her, the V/R variations are orbital phase-locked and coherent over more than 80 cycles (Štefl et al. 2007).

$\pi$ Aqr (HR 8539, HD 212571) is a bright, rapidly rotating ($\upsilon \sin i \approx 300 \mathrm{km\,s^{-1}}$) classical Be star with a variable mass loss. Analyzing its $H_\alpha$ line profiles and photospheric absorption during a diskless phase in 1996–2001, Bjorkman et al. (2002) suggested that $\pi$ Aqr is a binary system with an orbital period of $P_{orb} = 84.1$ days. The system consists of two stars with masses $M_1 \sin^3 i = 12.4 M_\odot$ and $M_2 \sin^3 i = 2.0 M_\odot$. The orbit is viewed at an inclination angle of $50° - 75°$. The components mass ratio and separation are $M_2/M_1 = 0.16$ and $a = 0.96 \sin^{-1} i$ AU, respectively. Using the evolutionary tracks from Schaerer et al. (1993), the effective temperature $T^1_{eff} = 24000 \pm 1000$ of the primary component, and its luminosity $\log(L_{bol}/L_\odot) = 4.1 \pm 0.3$, (Bjorkman et al. 2002) estimated the primary's mass to be $M_1 = 11 \pm 1.5 M\odot$. We further address this issue in Sect. 4.1.

Variability of the Balmer line profiles of $\pi$ Aqr, which appeared double-peaked most of the time, has been reported by McLaughlin (1962) and Pollmann (2012). McLaughlin (1962) observed strong V/R variations ranging from 0.5 to 4.0, and several periods of absence of bright emission lines (1936–1937, 1944–1945, 1950). Based on the $\pi$ Aqr spectra obtained between October 2004 and August 2011 together with the available spectra of the data base BeSS[1], Pollmann (2012) found a dominant frequency in the power spectrum of the V/R ratio that corresponded to a period of $83.8 \pm 0.8$ days. This value coincides within the errors with the above mentioned orbital period of the system.

In this paper we attempt a new period analysis of the V/R variations in the $H_\alpha$ line profile of $\pi$ Aqr based on spectroscopic observations obtained over ~40 orbital cycles of the system in 2004–2013. The disk structure of $\pi$ Aqr was probed using the Doppler tomography method. In Sect.2 we describe our observations, in Sect.3 period analysis of the $H_\alpha$ line profile variation is presented. The Doppler tomography of the system and modelling of the circumstellar disk are presented in Sect.4.2, and the results and conclusion are presented and discussed in Sect. 5.

[1] http:/basebe.obspm.fr/basebe

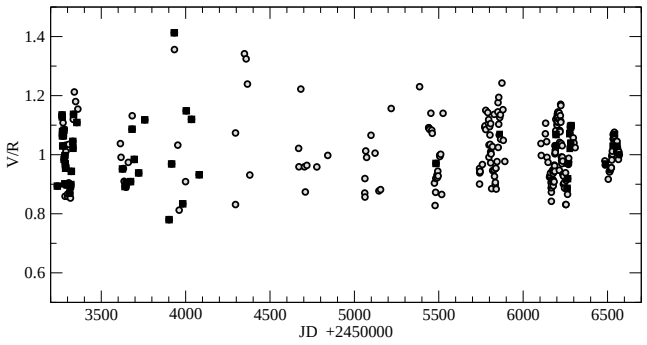


**Fig. 2.** Variation of V/R ratio of the $H_\alpha$ during reported observation.The amateur and professional data are marked by grey circles and black squares, respectively.

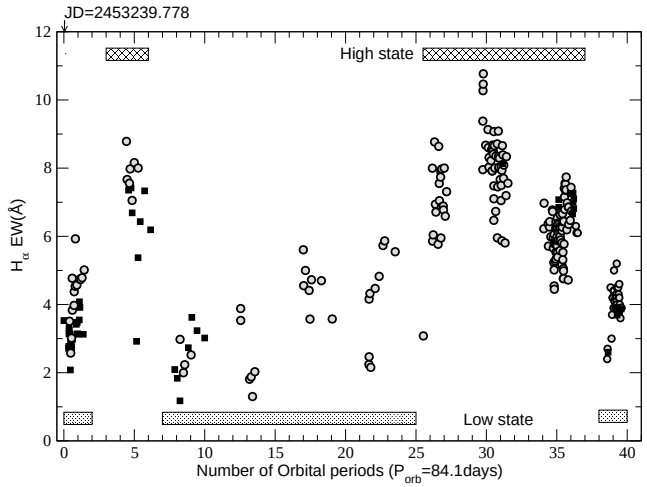


**Fig. 3.** The equivalent width of $H_\alpha$ emission line vs. of the orbital cycles of the system. The epoch of beginning of observations is shown too. The notes and bands in figure mark values of the $H_\alpha$ equivalent widths selected for "high" and "low" state. Symbols are the same as in Fig. 2.

## 2. Observations and data reduction

The object is continuously observed by both professionals and amateurs since its binarity was revealed. For this study we used spectra obtained by both communities. In particular, 36 spectra were obtained in 2004–2006 with the 1.0 m telescope of the Ritter Observatory of the University of Toledo (Toledo, OH, USA) using a fiber-fed échelle spectrograph with a Wright Instruments Ltd. CCD camera. The spectra consisted of nine non-overlapping orders ~ 70 Å in the range 5285–6597 Å with a spectral resolving power $R \simeq 26000$. Twelve spectra were obtained between October 2011–October 2013 at the 0.81 m telescope of the Three College Observatory (near Greensboro, NC, USA) using a fiber-fed échelle spectrograph manufactured by Shelyak Instruments with a SBIG ST–7XMEI (2011–2012) or an ATIK–460EX (2013) CCD camera. The spectra cover a range 4600–7200 Å with a $R \simeq 10000$. These data were reduced with IRAF[2].

The contribution of the amateur community to the campaign involved 17 observers from Germany, France, Spain, Mexico,

[2] IRAF is distributed by the National Optical Astronomy Observatories, which are operated by the Association of Universities for Research in Astronomy, Inc., under contract with the National Science Foundation.

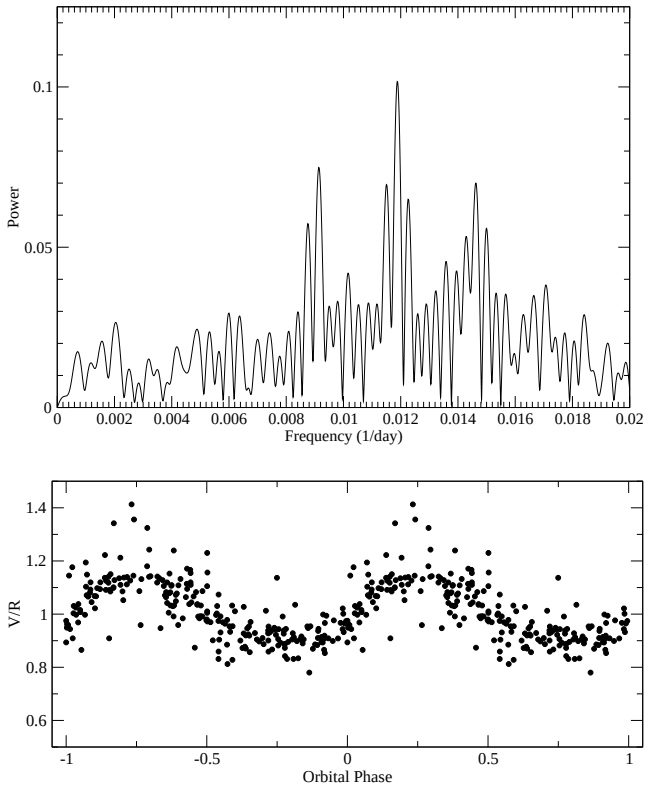


**Fig. 4.** Top panel: The power spectrum of V/R variation. Bottom panel: The V/R ratio folded on the orbital period of the system 84.1 day. $\phi_{orb} = 0.0$ corresponds to the inferior conjunction of the secondary.

Switzerland, and the USA. They used 0.2 m to 0.4 m telescopes with a long-slit (in most cases) and échelle spectrographs with a range of $R$ = 10000–22000. In total, 238 spectra were obtained between September 2004 and October 2013. Data reduction was performed using MaxIm-DL 3.06 (Diffraction Limited, Sehgal Corporation) for Pollmann's data, while data from other amateurs were reduced with software packages developed for amateur spectrographs, such as SpcAudace[3], Audela[4], VSpec[5], and IRIS3[6]. Spectral line parameters were measured with the spectral classification software package MK32[7]. No systematic difference in the V/R ratios or the $H_\alpha$ line equivalent widths (hereafter EW$_{H_\alpha}$) were found between the professional and amateur data (see Fig. 2 & 3). We showed earlier that radial velocity data from both communities also agree very well (Miroshnichenko et al. 2013). The dates of observations, the source, and results of the V/R and EW measurements are presented in Table 1, which is available in the online version.

## 3. Variability of the $H_\alpha$ line

As noted above, the $H_\alpha$ line profile of $\pi$ Aqr is double-peaked and strongly variable. Examples of the $H_\alpha$ line profile for two epochs of observations are shown in Figure 1. We measured the V/R ratio (defined as $V/R = I_V/I_R$) in the $H_\alpha$ emission line using peak intensities of the V and R components which were separately fitted with a single gaussian. The values of the V/R ratio vary in the range of 0.8 − 1.4 (Fig. 2) and do not correlate with EW$_{H_\alpha}$ (Fig. 3). The latter ranges between 1.0 and 11.0 Å and shows no periodicity. We refer to the spectra with a stronger $H_\alpha$ line (EW$_{H_\alpha} \geq$ 4.8Å) as to a "high state" and to those with a weaker $H_\alpha$ line as to a "low state" for the following analysis. The Discrete Fourier Transform (DFT) method[8] was used to search for periodicity in the V/R variation during our observations. The dominant frequency in the power spectrum is 0.011873±0.00028 day$^{-1}$ corresponds to a period of 84.2 ± 0.2 days that is in agreement with the system orbital period of $P_{orb}$ = 84.1 days found by Bjorkman et al. (2002). The resulting power spectrum and the V/R ratio folded with the dominant frequency are presented in Figure 4. Therefore, we conclude that the V/R variations in $\pi$ Aqr are locked with the orbital period, at least on a time scale of ≈ 3400 days or 40 orbital cycles. The shape of the V/R variation curve is sinusoidal.

## 4. Doppler tomography and Disk model.

### 4.1. System parameters

There is an apparent discrepancy between the dynamical and the evolutionary mass of the primary component that was outlined. This problem was not resolved by Bjorkman et al. (2002), therefore we reanalyzed below system parameters of the $\pi$ Aqr binary.

We calculated an absolute magnitude of $M_V = -2.96^{+0.50}_{-0.58}$ mag using the following: system brightness during the diskless epoch (1996–2001) of $V$ = 4.85 mag, an interstellar extinction of $A_V$ = 0.15 mag, and a *HIPPARCOS* distance $340^{+105}_{-70}$pc (Perryman & ESA 1997). A more recent distance $240^{+17}_{-15}$pc (van Leeuwen 2007) gives an absolute magnitude of $M_V = -2.20^{+0.15}_{-0.16}$ mag. Applying a bolometric correction of $BC_V = -2.36 \pm 0.10$ mag for $T_{\rm eff} = 24000 \pm 1000K$ (Miroshnichenko 1997), one gets a luminosity of log L/L$_\odot$ = 4.02 ± 0.24 for the larger distance and log L/L$_\odot$ = 3.72 ± 0.08 for the smaller one. These luminosities correspond to initial masses of 10.5 M$_\odot$ and 9.5 M$_\odot$, respectively, on the most recent evolutionary tracks with rotation by Ekström et al. (2012). Both these values are noticeably lower than the primary's dynamical mass $M_1 \sin^3 i = 12.4 M_\odot$ from Bjorkman et al. (2002). Since the radial velocity curves of both companions were well-established over the entire diskless period, the dynamical mass seems to be more reliable than the evolutionary mass. As seen in Fig.5 (left panel), the primary's mass ranges within 12.5—17.0 M$_\odot$ for the most probable orbital inclination of $i = 65-85^\circ$ (Bjorkman et al. 2002). This mass range requires a higher luminosity of the system (see Fig.5, right panel). Comparison with the evolutionary models by Ekström et al. (2012) also shows that the primary component with $T^1_{eff} = 24000K$ in $\pi$ Aqr has evolved out of the main-sequence if its mass exceeds ∼15 M$_\odot$.

As Be stars are considered to be main-sequence objects (e.g., Frémat et al. 2006), we therefore adopt a mass of 14.0±1.0 M$_\odot$ for the primary. This constrains its luminosity at log L/L$_\odot$ = 4.7 ± 0.1, which in turn leads to $M_V = -4.64 \pm 0.25$ mag and a distance of 740±90 pc. A separate study of stars near the object's line of sight (which is beyond the scope of this paper) is needed to verify this result. Nevertheless, the mass adjustment will only change the circumstellar disk scale, but not the qualitative results of our modelling. In Table 2 we present a summary of adopted parameters of the $\pi$ Aqr binary system.

[3] http://wsdiskovery.free.fr/spcaudace
[4] http://www.audela.org/dokuwiki/doku.php/en/start
[5] http://www.astrosurf.com/vdesnoux/download.html
[6] http://www.astrosurf.com/buil/isis/isis_en.htm
[7] http://www.appstate.edu/~grayro/MK/MKbook.html
[8] http://www.univie.ac.at/tops/Period04/

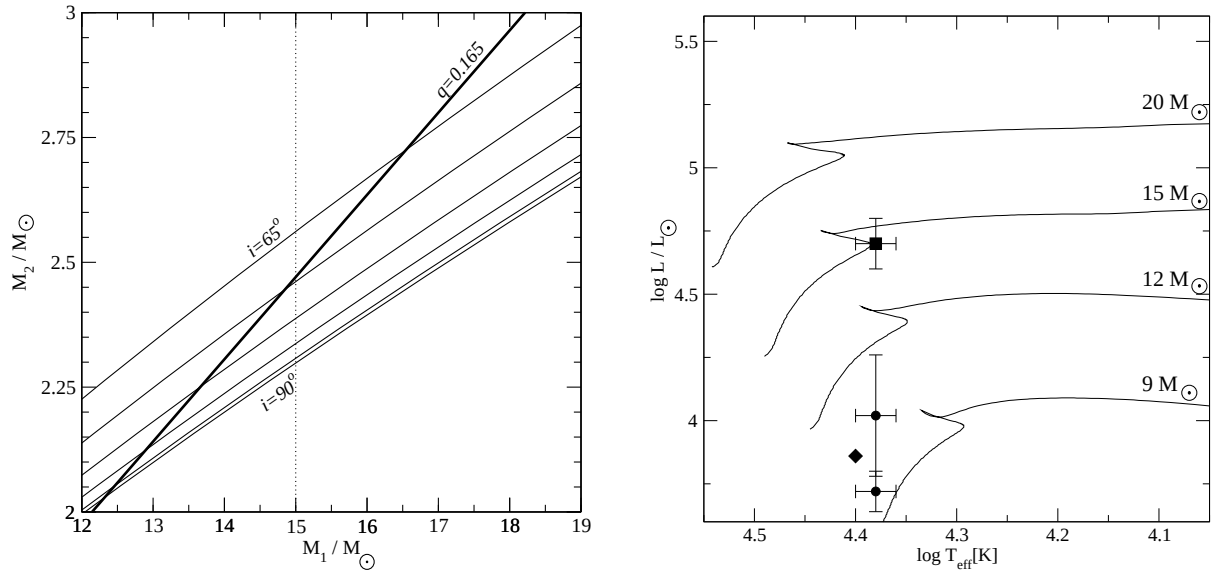


**Fig. 5.** Left panel: $M_2$ vs $M_1$ relationships for different inclination $i$ of the system orbital plane obtained from the mass function $f(M) = \frac{K_1^3 P_{orb}}{2\pi G} = 0.041 M_\odot$. The inclination range is of 65° — 90° with a step of 5° from top to bottom. The solid-line corresponds to a companions mass ratio of $q = 0.165$. Main-sequence stars with $T_{\rm eff} = 24000$K are located to the left from the dotted-line. Right panel: A Hertzsprung-Russell diagram with recent determinations of fundamental parameters of $\pi$ Aqr. Solid lines show evolutionary tracks of stars with rotation from Ekström et al. (2012). Initial masses are indicated by numbers at the corresponding track. Filled circles show the positions based on the luminosity calculated using the two *HIPPARCOS* distances (see text), the diamond shows data from Hohle et al. (2010), and the filled square shows parameters adopted here.

**Table 2.** Adopted parameters of $\pi$ Aqr.

| | |
|---|---|
| Period | 84.1(1) days |
| $M_1$ | 14.0(1.0) $M_\odot$ |
| $T^1_{eff}$ | 24000(1000) K |
| log $L/L_\odot$ | 4.7(1) |
| $R_1$* | 13.0(1.4)$R_\odot$ |
| $\upsilon_c$ | 453km s$^{-1}$ |
| $M_V$* | -4.64(25) |
| $q$ mass ratio | $\geq 0.165$ |
| $i$ system inclination | 65°-85° |
| $M_2$ | 2.31(16)$M_\odot$ |
| $a$ separation | 0.96 AU |
| Distance | 740(90) pc |

* based on $L/L_\odot$ and $T^1_{eff}$

numbers in brackets are $1\sigma$ uncertainties referring to last significant digits quoted

### 4.2. Doppler tomography

The $H_\alpha$ line profiles of $\pi$ Aqr were recorded at many orbital phases of the system over ~40 orbital cycles. Our finding that the V/R variations are locked with the orbital period suggests that the $H_\alpha$ line profile variability could be caused by a complex structure in the circumstellar disk. We used Doppler tomography (Marsh & Horne 1988) to study the structure of the disk around primary in $\pi$ Aqr.

The Doppler maps were built by combining time-resolved spectra using the maximum entropy method as implemented by Spruit (1998)[9]. Figure 6 shows phased time series spectra around the $H_\alpha$ line and corresponding Doppler maps of all spectra (top raw, left panel), "low" (bottom raw, left panel) and "high" (bottom raw, right panel) states, and a difference between each spectrum in a "high" and the average spectrum in the "low" state (top raw, right panel). The orbital period of $P_{\rm orb} = 84.1$ days, the primary mass of $M_1 = 14.0\,M_\odot$, and the mass ratio $q = 0.16$ (Table 2) are used to overlay positions of the stellar components on the Doppler maps. The inclination angle $i = 70°$ is arbitrarily chosen based on the discussion in Sect. 4.1. $\phi_{orb} = 0.0$ corresponds to the inferior conjunction of the secondary. The location of the main components in the system, such as the position of the centre of mass, the primary, the secondary, and the Roche lobe of the secondary star, are indicated.

The Doppler maps of all spectra show a non-uniform structure of the disk around the primary: a ring with the inner and outer radii at $V_{in} \approx 450$ km s$^{-1}$ and $V_{out} \approx 200$ km s$^{-1}$, respectively, together with an extended stable region (spot) at $V_x \approx 225$ km s$^{-1}$ and $V_y \approx 100$ km s$^{-1}$. We note that $EW_{H_\alpha}$ is a function of the total flux and surface brightness distribution of the disk. The "spot" is brighter and more extended in the "High" state compared to the "Low"" state. However, the brightness of the extended region is significantly lower than the total disk brightness and corresponds to an S-wave that can be seen only in "High-Low" trailed spectra. The disk radius of $\approx 65 R_\odot = 0.33$ AU was estimated assuming Keplerian motion of a particle in a circular orbit at the disk outer edge. Based on the results of the Doppler tomography, a geometrical model of the $\pi$ Aqr system is presented in Figure 7.

## 5. Discussion and Conclusion

In this paper we attempted a new period analysis of the V/R variations in the $H_\alpha$ line profile of $\pi$ Aqr and probe the primary's circumstellar disk structure based on spectroscopic observations obtained over multiple orbital cycles of the system. The main conclusions of our analysis are:

— The primary star has a mass of $M_1 = 14 \pm 0.1 M_\odot$ and a radius of $13.0 \pm 1.4 R_\odot$. The latter is nearly twice as

[9] http://www.mpa-garching.mpg.de/~henk/pub/dopmap

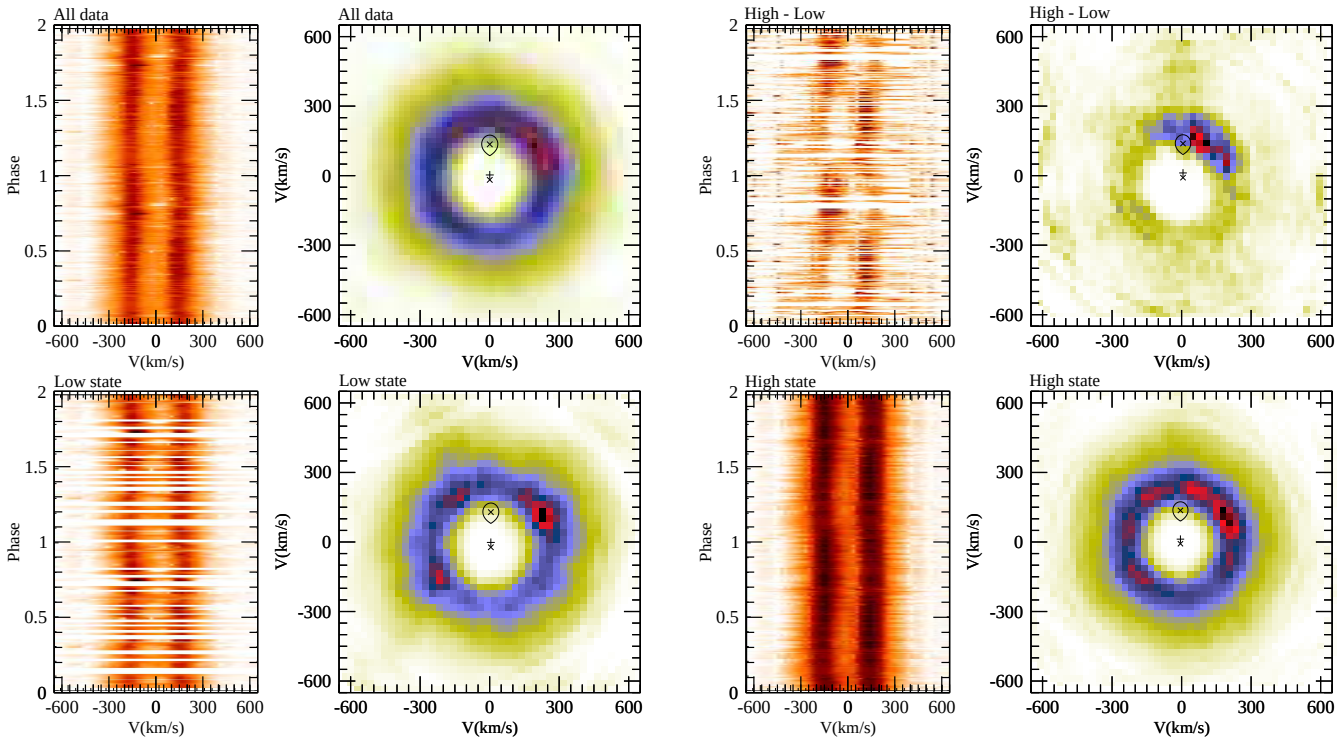


**Fig. 6.** The phased time series spectra around $H_\alpha$ line folded with the orbital period of the system and the corresponding Doppler maps are shown. The orbital period of $P_{orb}$ = 84.1 days, the primary mass of $M_1 = 14.0 M_\odot$ , and the mass ratio of q = 0.16 are used to overlay positions of the stellar components on the Doppler maps. The inclination angle $i = 70°$ is arbitrarily chosen based on suggestions by Bjorkman et al. (2002). $\phi_{orb} = 0.0$ corresponds to the inferior conjunction of the secondary.

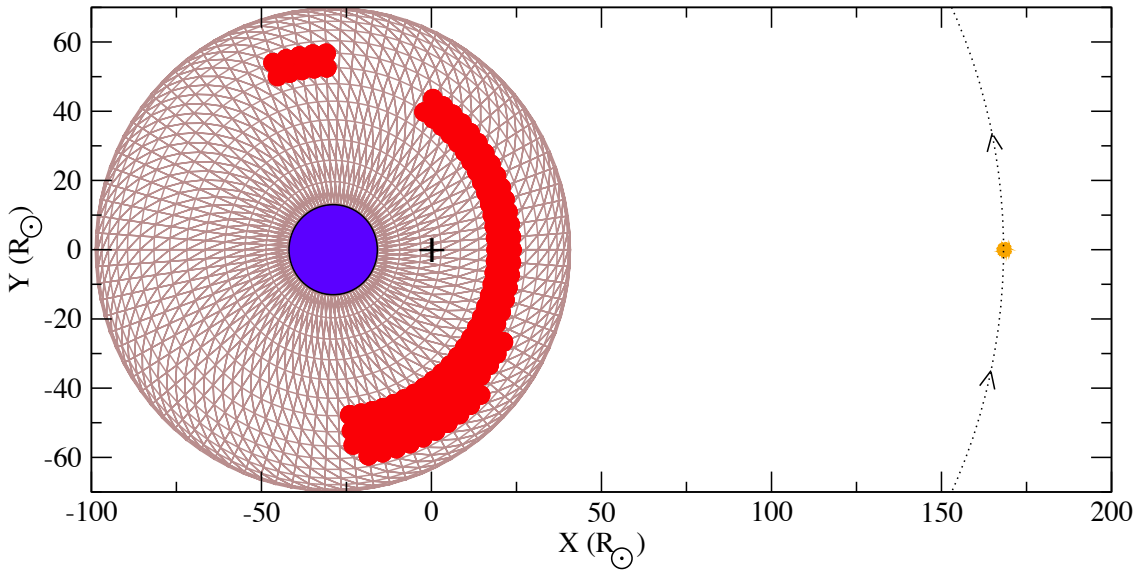


**Fig. 7.** Our geometrical model of $\pi$ Aqr. The blue and orange filled circles mark the primary and the secondary, respectively. The circumstellar disk is shown in brown colour. The red regions in the disk are constructed on the basis of the Doppler tomography and correspond the excess of $H_\alpha$ emission comparison with the rest of the disk. Scales of both axes are given in solar radii. Arrows show the direction of the binary rotation, and the cross indicates the centre of mass of the system. Parameters of the system are given in Table 2.

large as that of a ZAMS star with the same mass. The system orbit most likely has an inclination angle in the range of 65° – 85°.

— The V/R variations for the $H_\alpha$ line of $\pi$ Aqr show a sinusoidal behaviour with a period that coincides with the orbital period of the system. Therefore, based on the results of Bjorkman et al. (2002), Pollmann (2012), and the analysis presented here, we propose to include $\pi$ Aqr in the list of Be binaries that show orbital phase-locked V/R variations. The V/R variations reported here were coherent over ~40 cycles.

— There is an S-wave in the $H_\alpha$ phased time series spectra, and the Doppler tomograms demonstrate a corresponding bright extended spot within the circumstellar disk. The radius of the circumstellar disk around the primary component is $\sim 65R_\odot$. The spot is located in the outer part of the disk that faces the secondary. The position of the spot in the disk is stable, but its relative brightness correlates with the $EW_{H_\alpha}$ value. In general, the structure of the spot looks like a one-armed spiral density pattern. However, there is a faint hint of the second arm at the opposite side of the disk. The brightest part of the spot begins at $\approx -90^\circ$ from the major axis of the system and continues to $\sim 120^\circ$ counterclockwise with decreasing intensity (Figures 6 and 7).

Long-term V/R variations in Be stars are well explained by a model of global one-armed oscillations in the equatorial disk first proposed by Kato (1983) and developed by Okazaki (1991, 1997). In this model the one-armed perturbation slowly (on a time scale of $\sim$ 10 years) precesses in the opposite direction to the semi-Keplerian motion as a result of pressure forces in the disk. If we take into account deviation from a $1/r$ point potential, this leads to a slowly revolving prograde oscillation mode also with a very long time scale semi-periods (Papaloizou et al. 1992). The following studies include other effects, although the number of free parameters and their large range lead to a low predictive power of these models (Fiřt & Harmanec 2006).

A significant number of Be stars are binary systems (Porter & Rivinius 2003; Oudmaijer & Parr 2010; Miroshnichenko 2011). Nevertheless, in the current models, the oscillation period weakly depends on the orbital parameters. For example, Oktariani & Okazaki (2009) found that the oscillation period increases with increasing binary separation and/or decreasing binary mass ratio. However, two well-established examples of orbital phase-locked systems 4 Her and $\pi$ Aqr have relatively large separations and small mass ratios of 0.06–0.016 (Koubsky et al. 1997) and 0.165 (Bjorkman et al. 2002), respectively. Therefore, we must emphasize that, in fact, a number of Be systems exist with phase-locked V/R variations. Unfortunately, no explanation currently exists for this phenomenon within the framework of the one-armed oscillation model. It is likely that careful accounting of tidal or/and heating effects from the secondary on the structure of a circumstellar disk can improve the situation.

There are also a number of Be + sdO binaries, such as 59 Cyg (Maintz et al. 2005; Peters et al. 2013), FY CMa (Štefl et al. 2005; Peters et al. 2008) and $\phi$ Per (Gies et al. 1993; Štefl et al. 2000)), in which the $V/R$ variations are also locked with the orbital period. The orbital period locked emission in these systems is more likely originated in the outer parts of the Be star disk facing the secondary that are directly heated by a low mass ($\log M/M_\odot$ from $\sim -0.1$ to $\sim 0.1$), hot ($\log T_{\rm eff} \sim 4.7$) subdwarf (sdO) companion (Peters et al. 2013, see Table 5). Most sdO/sdB stars have masses between 0.40 $M_\odot$ and 0.55 $M_\odot$, but some of them may be as massive as $\sim 1.1M_\odot$ (Zhang et al. 2010). Although the effective temperature of the secondary component in $\pi$ Aqr is unknown, its mass $M_2$ can not be lower than 2 $M_\odot$ (Figure 5, left panel). Therefore, it is unlikely to be an sdO or sdB star.

Bjorkman et al. (2002) suggest that the secondary component in $\pi$ Aqr is probably an A– or F–type main-sequence star, since only signs of the primary component are seen in the UV spectrum. Nevertheless, the latter does not exclude that the mechanism of phase-locked $V/R$ variations in $\pi$ Aqr can be similar or the same (some tidal and heating effects on the structure of the circumstellar disk caused by the secondary) as that discussed above for Be + sdO binaries.

In any case, it is very important to continue observing $\pi$ Aqr and other phase-locked systems spectroscopically, photometrically, and interferometrically to search for more clues to them nature. Finally, the data, presented in this paper, manifest a further increasing role of the amateur spectroscopy in stellar astrophysics (cf., Miroshnichenko et al. 2013).

*Acknowledgements.* This work was supported by DGAPA/PAPIIT project IN 103912. A.M. acknowledges financial support from the University of North Carolina at Greensboro and from its Department of Physics and Astronomy. We thank observers at the Ritter Observatory for taking the spectra and reducing them. This work has made use of the BeSS database, operated at LESIA, Observatoire de Meudon, France: http://basebe.obspm.fr.

## References

Bjorkman, K. S., Miroshnichenko, A. S., McDavid, D., & Pogrosheva, T. M. 2002, ApJ, 573, 812
Bozic, H., Harmanec, P., Horn, J., et al. 1995, A&A, 304, 235
Carciofi, A. C., Okazaki, A. T., Le Bouquin, J.-B., et al. 2009, A&A, 504, 915
Doazan, V., Harmanec, P., Koubsky, P., Krpata, J., & Zdarsky, F. 1982, A&A, 115, 138
Ekström, S., Georgy, C., Eggenberger, P., et al. 2012, A&A, 537, A146
Fiřt, R. & Harmanec, P. 2006, A&A, 447, 277
Frémat, Y., Neiner, C., Hubert, A.-M., et al. 2006, A&A, 451, 1053
Gies, D. R., Bagnuolo, Jr., W. G., Baines, E. K., et al. 2007, ApJ, 654, 527
Gies, D. R., Bagnuolo, Jr., W. G., Ferrara, E. C., et al. 1998, ApJ, 493, 440
Gies, D. R., Willis, C. Y., Penny, L. R., & McDavid, D. 1993, PASP, 105, 281
Grzenia, B. J., Tycner, C., Jones, C. E., et al. 2013, AJ, 145, 141
Harmanec, P., Koubský, P., Krpata, J., & Zdárský, F. 1976, Bulletin of the Astronomical Institutes of Czechoslovakia, 27, 47
Hohle, M. M., Neuhäuser, R., & Schutz, B. F. 2010, Astronomische Nachrichten, 331, 349
Juza, K., Harmanec, P., Hill, G. M., Tarasov, A. E., & Matthews, J. M. 1991, Bulletin of the Astronomical Institutes of Czechoslovakia, 42, 39
Kato, S. 1983, PASJ, 35, 249
Koubsky, P., Harmanec, P., Kubat, J., et al. 1997, A&A, 328, 551
Maintz, M., Rivinius, T., Stahl, O., Stefl, S., & Appenzeller, I. 2005, Publications of the Astronomical Institute of the Czechoslovak Academy of Sciences, 93, 21
Marsh, T. R. & Horne, K. 1988, MNRAS, 235, 269
McLaughlin, D. B. 1962, ApJS, 7, 65
Mennickent, R. E., Sterken, C., & Vogt, N. 1997, A&A, 326, 1167
Miroshnichenko, A. S. 1997, in IAU Symposium, Vol. 189, IAU Symposium, ed. T. R. Bedding, A. J. Booth, & J. Davis, 50P
Miroshnichenko, A. S. 2011, in IAU Symposium, Vol. 272, IAU Symposium, ed. C. Neiner, G. Wade, G. Meynet, & G. Peters, 304–305
Miroshnichenko, A. S., Pasechnik, A. V., Manset, N., et al. 2013, ApJ, 766, 119
Okazaki, A. T. 1991, PASJ, 43, 75
Okazaki, A. T. 1997, A&A, 318, 548
Oktariani, F. & Okazaki, A. T. 2009, PASJ, 61, 57
Oudmaijer, R. D. & Parr, A. M. 2010, MNRAS, 405, 2439
Papaloizou, J. C., Savonije, G. J., & Henrichs, H. F. 1992, A&A, 265, L45
Perryman, M. A. C. & ESA, eds. 1997, ESA Special Publication, Vol. 1200, The HIPPARCOS and TYCHO catalogues. Astrometric and photometric star catalogues derived from the ESA HIPPARCOS Space Astrometry Mission
Peters, G. J. 1972, PASP, 84, 334
Peters, G. J., Gies, D. R., Grundstrom, E. D., & McSwain, M. V. 2008, ApJ, 686, 1280
Peters, G. J., Pewett, T. D., Gies, D. R., Touhami, Y. N., & Grundstrom, E. D. 2013, ApJ, 765, 2
Pollmann, E. 2012, Information Bulletin on Variable Stars, 6023, 1
Porter, J. M. & Rivinius, T. 2003, PASP, 115, 1153
Quirrenbach, A., Bjorkman, K. S., Bjorkman, J. E., et al. 1997, ApJ, 479, 477
Rivinius, T., Štefl, S., & Baade, D. 1999, A&A, 348, 831
Rivinius, T., Štefl, S., Maintz, M., Stahl, O., & Baade, D. 2004, A&A, 427, 307
Schaerer, D., Charbonnel, C., Meynet, G., Maeder, A., & Schaller, G. 1993, A&AS, 102, 339
Spruit, H. C. 1998, ArXiv Astrophysics e-prints
Struve, O. 1931, ApJ, 73, 94
Štefl, S., Hummel, W., & Rivinius, T. 2000, A&A, 358, 208
Štefl, S., Okazaki, A. T., Rivinius, T., & Baade, D. 2007, in Astronomical Society of the Pacific Conference Series, Vol. 361, Active OB-Stars: Laboratories for Stellare and Circumstellar Physics, ed. A. T. Okazaki, S. P. Owocki, & S. Stefl, 274
Štefl, S., Rivinius, T., Baade, D., Maintz, M., & Stahl, O. 2005, in Astronomical Society of the Pacific Conference Series, Vol. 337, The Nature and Evolution of Disks Around Hot Stars, ed. R. Ignace & K. G. Gayley, 309
van Leeuwen, F. 2007, A&A, 474, 653
Zhang, X., Chen, X., & Han, Z. 2010, Ap&SS, 329, 11

**Table 1.** The dates of observations of $\pi$ Aqr, the source, and results of V/R and EW measurements of $H_\alpha$ emission line.

| HJD | $V/R_{H_\alpha}$ | $EW_{H_\alpha}$ | Reference |
|---|---|---|---|
| 2453239.78 | 0.89 | 3.53 | 1 |
| 2453267.69 | 1.13 | 2.71 | 1 |
| 2453268.64 | 1.13 | 2.77 | 1 |
| 2453269.67 | 1.06 | 3.14 | 1 |
| 2453270.64 | 1.08 | 3.31 | 1 |
| 2453271.72 | 1.03 | 3.25 | 1 |
| 2453273.38 | 1.04 | 3.51 | 2 |
| 2453275.60 | 1.06 | 3.14 | 1 |
| 2453278.66 | 1.08 | 2.08 | 1 |
| 2453279.66 | 0.98 | 2.95 | 1 |
| 2453280.57 | 1.02 | 2.58 | 2 |
| 2453283.67 | 0.90 | 2.80 | 1 |
| 2453284.64 | 1.00 | 3.01 | 1 |
| 2453285.41 | 0.98 | 3.01 | 2 |
| 2453286.67 | 0.97 | 2.74 | 1 |
| 2453288.67 | 0.95 | 2.96 | 1 |
| 2453289.45 | 1.00 | 2.99 | 2 |
| 2453289.59 | 0.95 | 4.77 | 1 |
| 2453290.30 | 1.00 | 3.83 | 2 |
| 2453297.54 | 0.98 | 3.93 | 2 |
| 2453300.35 | 0.96 | 3.97 | 2 |
| 2453301.41 | 0.96 | 4.38 | 2 |
| 2453307.39 | 0.97 | 4.54 | 2 |
| 2453308.31 | 1.01 | 5.93 | 2 |
| 2453313.62 | 0.87 | 3.42 | 1 |
| 2453316.57 | 0.89 | 3.13 | 1 |
| 2453317.21 | 0.97 | 4.57 | 2 |
| 2453319.58 | 0.90 | 3.48 | 1 |
| 2453322.53 | 0.94 | 3.14 | 1 |
| 2453331.57 | 1.05 | 3.55 | 1 |
| 2453332.58 | 1.02 | 4.08 | 1 |
| 2453334.19 | 1.03 | 4.74 | 2 |
| 2453335.54 | 1.14 | 3.91 | 1 |
| 2453340.18 | 1.05 | 4.74 | 2 |
| 2453348.20 | 1.04 | 4.78 | 2 |
| 2453355.52 | 1.11 | 3.13 | 1 |
| 2453361.21 | 1.04 | 5.01 | 2 |
| 2453613.35 | 1.02 | 8.78 | 2 |
| 2453617.28 | 0.99 | 7.67 | 2 |
| 2453625.66 | 0.95 | 7.35 | 1 |
| 2453631.20 | 0.98 | 7.56 | 2 |
| 2453635.29 | 0.97 | 7.98 | 2 |
| 2453640.70 | 0.89 | 7.42 | 1 |
| 2453647.31 | 0.96 | 6.69 | 2 |
| 2453647.61 | 0.90 | 6.69 | 1 |
| 2453660.29 | 0.98 | 8.16 | 2 |
| 2453673.56 | 0.91 | 2.92 | 1 |
| 2453682.61 | 1.09 | 5.37 | 1 |
| 2453683.21 | 1.05 | 8.00 | 2 |
| 2453695.59 | 0.98 | 6.43 | 1 |
| 2453757.54 | 1.12 | 6.19 | 1 |
| 2453901.84 | 0.78 | 2.09 | 1 |
| 2453916.83 | 0.97 | 1.83 | 1 |
| 2453932.83 | 1.41 | 1.17 | 1 |
| 2453933.55 | 1.08 | 2.98 | 2 |
| 2453953.56 | 1.01 | 2.00 | 2 |
| 2453961.52 | 0.96 | 2.23 | 2 |
| 2453982.70 | 0.83 | 2.73 | 1 |
| 2453999.38 | 0.98 | 2.52 | 2 |

| | | | |
|---|---|---|---|
| 2454003.65 | 1.15 | 3.62 | 1 |
| 2454034.67 | 1.12 | 3.23 | 1 |
| 2454080.49 | 0.93 | 3.02 | 1 |
| 2454295.55 | 0.96 | 3.88 | 2 |
| 2454295.58 | 1.02 | 3.53 | 2 |
| 2454348.40 | 1.05 | 1.81 | 2 |
| 2454358.44 | 1.07 | 1.88 | 2 |
| 2454366.36 | 1.03 | 1.30 | 2 |
| 2454380.35 | 0.99 | 2.03 | 2 |
| 2454669.49 | 1.01 | 5.61 | 2 |
| 2454671.47 | 0.99 | 4.55 | 2 |
| 2454682.50 | 1.03 | 5.00 | 2 |
| 2454704.41 | 0.99 | 4.41 | 2 |
| 2454709.37 | 0.97 | 3.57 | 2 |
| 2454718.42 | 0.99 | 4.73 | 2 |
| 2454777.35 | 0.99 | 4.70 | 2 |
| 2454842.23 | 1.00 | 3.58 | 2 |
| 2455061.39 | 0.97 | 2.24 | 2 |
| 2455062.44 | 0.98 | 4.16 | 2 |
| 2455062.56 | 0.97 | 2.47 | 2 |
| 2455067.39 | 0.99 | 4.32 | 2 |
| 2455072.41 | 1.00 | 2.16 | 2 |
| 2455098.38 | 1.01 | 4.47 | 2 |
| 2455122.48 | 1.01 | 4.83 | 2 |
| 2455145.30 | 0.97 | 5.73 | 2 |
| 2455155.26 | 0.95 | 5.87 | 2 |
| 2455218.26 | 1.05 | 5.55 | 2 |
| 2455386.55 | 1.07 | 3.08 | 2 |
| 2455440.39 | 1.04 | 8.00 | 2 |
| 2455441.45 | 1.03 | 5.86 | 2 |
| 2455445.37 | 1.03 | 6.04 | 2 |
| 2455453.33 | 1.05 | 8.77 | 2 |
| 2455458.44 | 1.03 | 6.94 | 2 |
| 2455461.32 | 1.03 | 6.71 | 2 |
| 2455474.31 | 0.97 | 5.77 | 2 |
| 2455478.28 | 0.92 | 8.64 | 2 |
| 2455481.28 | 0.95 | 7.55 | 2 |
| 2455482.29 | 0.97 | 7.05 | 2 |
| 2455489.46 | 0.97 | 7.74 | 2 |
| 2455491.31 | 0.97 | 5.95 | 2 |
| 2455494.29 | 0.98 | 6.86 | 2 |
| 2455496.34 | 0.96 | 7.97 | 2 |
| 2455505.42 | 1.00 | 6.89 | 2 |
| 2455506.40 | 0.99 | 6.77 | 2 |
| 2455511.46 | 1.00 | 8.00 | 2 |
| 2455517.25 | 0.95 | 6.59 | 2 |
| 2455525.35 | 1.06 | 7.31 | 2 |
| 2455741.58 | 0.97 | 7.96 | 2 |
| 2455741.65 | 0.98 | 9.38 | 2 |
| 2455742.60 | 0.97 | 10.27 | 2 |
| 2455743.66 | 0.97 | 10.46 | 2 |
| 2455744.65 | 0.97 | 10.77 | 2 |
| 2455758.49 | 0.98 | 8.67 | 2 |
| 2455772.50 | 1.03 | 9.13 | 2 |
| 2455774.55 | 1.05 | 8.60 | 2 |
| 2455778.48 | 1.04 | 8.03 | 2 |
| 2455778.53 | 1.06 | 8.31 | 2 |
| 2455790.49 | 1.06 | 8.22 | 2 |
| 2455794.46 | 1.04 | 8.54 | 2 |
| 2455795.45 | 1.04 | 8.53 | 2 |
| 2455797.39 | 1.00 | 7.91 | 2 |
| 2455797.54 | 1.02 | 7.92 | 2 |
| 2455801.46 | 1.03 | 8.68 | 2 |
| 2455803.39 | 1.02 | 8.51 | 2 |

| | | | |
|---|---|---|---|
| 2455803.46 | 1.01 | | 2 |
| 2455804.49 | 1.00 | 8.41 | 2 |
| 2455807.45 | 1.05 | 6.47 | 2 |
| 2455807.45 | 1.01 | 7.48 | 2 |
| 2455807.52 | 0.99 | 9.07 | 2 |
| 2455810.35 | 1.01 | 8.66 | 2 |
| 2455813.39 | 0.98 | 8.00 | 2 |
| 2455818.41 | 1.01 | 6.73 | 2 |
| 2455819.44 | 0.99 | 8.36 | 2 |
| 2455827.53 | 1.01 | 8.71 | 2 |
| 2455828.34 | 1.05 | 5.96 | 2 |
| 2455830.37 | 0.97 | 7.45 | 2 |
| 2455834.31 | 0.95 | 9.09 | 2 |
| 2455835.37 | 0.98 | 8.34 | 2 |
| 2455837.45 | 0.98 | 8.00 | 2 |
| 2455838.36 | 0.99 | 8.03 | 2 |
| 2455840.40 | 0.96 | 8.29 | 2 |
| 2455845.36 | 0.99 | 7.67 | 2 |
| 2455850.29 | 1.06 | 7.05 | 2 |
| 2455851.26 | 1.06 | 7.49 | 2 |
| 2455852.32 | 1.01 | 8.05 | 2 |
| 2455855.28 | 1.08 | 5.87 | 2 |
| 2455855.37 | 1.05 | 7.93 | 2 |
| 2455858.39 | 1.04 | 8.66 | 2 |
| 2455860.69 | 1.07 | 8.13 | 3 |
| 2455861.37 | 1.04 | 8.39 | 2 |
| 2455865.28 | 1.07 | 7.70 | 2 |
| 2455866.52 | 1.04 | 8.09 | 2 |
| 2455874.29 | 1.10 | 5.81 | 2 |
| 2455880.36 | 1.07 | 7.19 | 2 |
| 2455882.27 | 1.02 | 8.34 | 2 |
| 2455891.39 | 0.99 | 7.56 | 2 |
| 2456105.63 | 1.01 | 6.22 | 2 |
| 2456107.62 | 0.99 | 6.97 | 2 |
| 2456131.54 | 1.04 | 6.36 | 2 |
| 2456133.45 | 1.04 | 5.71 | 2 |
| 2456139.47 | 1.02 | 6.27 | 2 |
| 2456141.50 | 1.01 | 6.43 | 2 |
| 2456147.55 | 0.99 | 5.99 | 2 |
| 2456156.52 | 0.97 | 6.77 | 2 |
| 2456158.47 | 0.97 | 6.73 | 2 |
| 2456162.43 | 0.98 | 5.96 | 2 |
| 2456162.45 | 0.97 | 5.65 | 2 |
| 2456165.44 | 0.97 | 5.23 | 2 |
| 2456167.37 | 0.95 | 5.78 | 2 |
| 2456167.44 | 0.95 | 5.01 | 2 |
| 2456167.46 | 0.95 | 4.54 | 2 |
| 2456167.47 | 0.94 | 6.06 | 2 |
| 2456168.41 | 0.95 | 4.45 | 2 |
| 2456172.38 | 0.96 | 5.82 | 2 |
| 2456174.39 | 0.98 | 5.27 | 2 |
| 2456177.32 | 0.96 | 5.76 | 2 |
| 2456177.40 | 0.99 | 5.90 | 2 |
| 2456177.50 | 0.98 | 6.23 | 2 |
| 2456178.37 | 0.96 | 6.22 | 2 |
| 2456178.43 | 0.96 | 5.33 | 2 |
| 2456178.47 | 0.98 | 6.42 | 2 |
| 2456179.35 | 0.96 | 5.54 | 2 |
| 2456180.45 | 0.97 | 5.53 | 2 |
| 2456183.34 | 0.96 | 5.98 | 2 |
| 2456185.32 | 0.98 | 5.72 | 2 |
| 2456186.36 | 0.99 | 6.54 | 2 |
| 2456186.42 | 0.98 | 6.23 | 2 |
| 2456187.31 | 0.98 | 5.54 | 2 |

| | | | |
|---|---|---|---|
| 2456188.35 | 0.99 | 5.39 | 2 |
| 2456188.41 | 1.00 | 5.88 | 2 |
| 2456190.35 | 1.01 | 6.13 | 2 |
| 2456190.41 | 1.00 | 6.39 | 2 |
| 2456193.30 | 1.02 | 6.35 | 2 |
| 2456193.45 | 1.04 | 5.90 | 2 |
| 2456194.64 | 1.03 | 6.85 | 3 |
| 2456200.34 | 1.04 | 6.28 | 2 |
| 2456200.61 | 1.06 | 6.16 | 2 |
| 2456202.42 | 1.05 | 5.58 | 2 |
| 2456203.45 | 1.05 | 6.00 | 2 |
| 2456204.33 | 1.05 | 6.63 | 2 |
| 2456204.40 | 1.05 | 5.87 | 2 |
| 2456205.34 | 1.06 | 6.24 | 2 |
| 2456206.29 | 1.06 | 5.89 | 2 |
| 2456213.40 | 1.05 | 5.81 | 2 |
| 2456213.46 | 1.04 | 5.16 | 2 |
| 2456214.40 | 1.05 | 6.16 | 2 |
| 2456216.39 | 1.02 | 6.27 | 2 |
| 2456217.33 | 1.04 | 6.43 | 2 |
| 2456217.38 | 1.02 | 6.66 | 2 |
| 2456219.27 | 1.03 | 5.31 | 2 |
| 2456220.37 | 1.06 | 5.53 | 2 |
| 2456222.26 | 1.05 | 4.76 | 2 |
| 2456222.34 | 1.03 | 5.05 | 2 |
| 2456223.29 | 1.05 | 4.99 | 2 |
| 2456223.43 | 1.04 | 4.76 | 2 |
| 2456225.42 | 1.01 | 6.44 | 2 |
| 2456226.35 | 0.99 | 5.77 | 2 |
| 2456228.26 | 0.99 | 7.41 | 2 |
| 2456229.37 | 0.99 | 7.15 | 2 |
| 2456231.35 | 1.00 | 6.79 | 2 |
| 2456232.35 | 1.00 | 7.55 | 2 |
| 2456234.35 | 1.00 | 7.35 | 2 |
| 2456235.24 | 0.98 | 7.53 | 2 |
| 2456238.30 | 0.95 | 7.36 | 2 |
| 2456239.30 | 0.98 | 7.74 | 2 |
| 2456243.24 | 0.96 | 6.19 | 2 |
| 2456245.27 | 0.95 | 6.98 | 2 |
| 2456251.31 | 0.97 | 4.72 | 2 |
| 2456252.28 | 0.95 | 6.86 | 2 |
| 2456254.20 | 0.96 | 6.86 | 2 |
| 2456254.32 | 0.95 | 6.35 | 2 |
| 2456263.35 | 0.96 | 6.47 | 2 |
| 2456263.48 | 0.97 | 7.26 | 3 |
| 2456268.30 | 0.99 | 7.44 | 2 |
| 2456270.34 | 0.99 | | 2 |
| 2456270.35 | 0.99 | 6.74 | 2 |
| 2456276.48 | 1.02 | 6.67 | 3 |
| 2456280.48 | 1.04 | 7.00 | 3 |
| 2456284.46 | 1.04 | 6.81 | 3 |
| 2456297.23 | 1.06 | 6.30 | 2 |
| 2456297.29 | 1.03 | | 2 |
| 2456301.28 | 1.04 | 6.10 | 2 |
| 2456308.25 | 1.02 | 6.10 | 2 |
| 2456484.50 | 0.98 | 2.40 | 2 |
| 2456486.56 | 0.97 | 2.70 | 2 |
| 2456489.70 | 0.97 | 2.60 | 3 |
| 2456504.42 | 0.92 | 4.50 | 2 |
| 2456510.38 | 0.94 | 3.00 | 2 |
| 2456513.50 | 0.94 | 3.70 | 2 |
| 2456516.43 | 0.95 | 4.20 | 2 |
| 2456518.38 | 0.95 | 4.20 | 2 |
| 2456522.39 | 0.96 | 3.90 | 2 |

| | | | |
|---|---|---|---|
| 2456522.44 | 0.96 | 4.40 | 2 |
| 2456525.37 | 1.00 | 5.00 | 2 |
| 2456525.44 | 0.98 | 4.40 | 2 |
| 2456528.43 | 1.00 | 4.10 | 2 |
| 2456528.44 | 1.01 | 4.10 | 2 |
| 2456530.71 | 1.03 | 3.92 | 3 |
| 2456533.39 | 1.07 | | 2 |
| 2456534.43 | 1.05 | 4.20 | 2 |
| 2456534.79 | 1.05 | 3.90 | 2 |
| 2456536.76 | 1.04 | | 2 |
| 2456538.42 | 1.06 | 4.30 | 2 |
| 2456539.43 | 1.07 | 4.20 | 2 |
| 2456539.45 | 1.07 | 4.20 | 2 |
| 2456540.42 | 1.08 | 4.10 | 2 |
| 2456541.35 | 1.05 | 5.20 | 2 |
| 2456541.40 | 1.04 | 4.50 | 2 |
| 2456541.44 | 1.04 | 4.00 | 2 |
| 2456543.63 | 1.07 | 3.69 | 3 |
| 2456549.75 | 1.05 | 4.50 | 2 |
| 2456550.82 | 1.02 | | 2 |
| 2456552.47 | 1.05 | 4.30 | 2 |
| 2456554.29 | 1.01 | 4.20 | 2 |
| 2456556.46 | 1.03 | 4.60 | 2 |
| 2456556.47 | 1.05 | 4.20 | 2 |
| 2456557.45 | 1.02 | | 2 |
| 2456558.57 | 1.03 | 3.77 | 3 |
| 2456559.41 | 1.02 | 4.00 | 2 |
| 2456560.43 | 1.01 | | 2 |
| 2456561.30 | 1.01 | | 2 |
| 2456563.39 | 1.01 | 3.60 | 2 |
| 2456564.69 | 0.98 | 3.90 | 2 |
| 2456567.34 | 1.01 | 3.90 | 2 |
| 2456567.58 | 1.00 | 3.87 | 3 |
| 2456569.69 | 1.00 | 3.90 | 2 |
| 2456570.62 | 1.01 | 3.80 | 3 |

**Notes.** 1 - Ritter Observatory; 2 - amateur data; 3 - Three College Observatory